

***BVRI* Photometry of the CX Cephei System (WR 151)**

KATE HUTTON

Seismological Laboratory, Caltech 252-21, Pasadena, CA 91125; katehutton@gmail.com

ARNE HENDEN

AAVSO, Cambridge, MA 02138; arne@aavso.org

DIRK TERRELL

Dept. of Space Studies, Southwest Research Institute, Boulder, CO 80302; terrell@boulder.swri.edu

Received 2009 April 11; accepted 2009 May 29; published 2009 June 26

ABSTRACT. We have obtained 699 new *BVRI* observations of the O5 + WN5 eclipsing binary system CX Cephei (WR 151), plus 126 more observations in *V* only. Our light curves are consistent with previous studies, showing a primary minimum (where the O5 star is eclipsed) of approximately 0.1 mag depth and a much smaller secondary minimum with an approximately 0.03 mag depth. Using the PHOEBE interface to the Wilson-Devinney computer code, we were able to obtain a reasonably satisfactory fit to these data, ignoring any possible contribution from atmospheric eclipse phenomena. The best-fit solution has $i = 61.1^\circ$ and results in masses of $36.8 M_\odot$ for the O5 star and $26.4 M_\odot$ for the Wolf-Rayet (WR) star. The binary system is detached. There is an asymmetry in the light curve, suggesting that the “leading side” of the O5 star (or the trailing side of the WR star) is brighter than vice versa. We also observed some features in the light curve that were persistent, but which we could not model. $O - C$ residuals relative to the PHOEBE fit reveal time variations with a total range of approximately 12% of the flux. Comparing our data with those of Lipunova & Cherpashchuk (1982), we find that the secondary minimum is less prominent today than it was in the 1980s. We were able to revise their period estimate to 2.12691 days.

1. INTRODUCTION

Wolf-Rayet (WR) stars are thought to be the remnant cores of the largest-mass stars, after a great deal of mass loss has dispersed the stars’ outer envelopes to expose the nuclear-processed material (e.g., Abbot & Conti 1987, Crowther 2007). Their spectra are characterized by strong, high-excitation emission lines of He, C, N, or O, with no absorption lines apparent. A commonly suggested evolutionary path begins with an early O V star ($>40 M_\odot$), whose extreme mass loss creates a luminous blue variable (LBV) and eventually a WR star. As with all the massive stars, the end point of the evolution is expected to be a supernova. Some theorists have suggested that the lack of a stellar envelope is a necessary condition for a Type Ib/c supernova with a gamma ray burst (GRB). WR stars are thus exotic and interesting stars.

WR stars are also quite rare (as are high-mass stars in general): 227 of them are known in our Galaxy, with 123 additional known in the Magellanic Clouds (van der Hucht 2001). Over 43% are estimated to be members of WR + O binaries (Moffat et al. 1976), but only a few are double-lined spectroscopic eclipsing binaries, from which we can learn something of the basic properties of the component stars. One of these few is CX Cephei.

The CX Cep system consists of an O5V star and a WN5 component (Lewis et al. 1993). Lipunova & Cherepashchuk (1982) used their own photometric observations and data from Hiltner (1948), between JD 2,444,394 to 2,444,514, to determine a period of 2.12687 days, the second shortest known (after CQ Cep) among WR + O binaries. The eclipses are shallow, approximately 0.1 mag in depth in *V*. Lewis et al. (1993), and earlier Massey & Conti (1981), performed spectroscopic analysis, yielding radial velocities for both components (using the $\lambda 4603$ N V emission line for the WR star and Balmer absorption lines for the O star), showing that the WR, or its envelope/wind, is in front during primary eclipse. Their analysis yields $M_O \sin^3 i = 25.2 \pm 1.9 M_\odot$ and $M_{WR} \sin^3 i = 17.8 \pm 1.4 M_\odot$. Estimates of the orbital inclination (i) vary from the 50° to 56° range, from light curve analysis by Lipunova & Cherepashchuk (1982), to 74° , from polarimetry measurements by Schulte-Ladbeck & van der Hucht (1989). For their modeling, Lipunova & Cherepashchuk incorporate atmospheric eclipsing, by the extended atmosphere/wind of the WR star. They conclude that the “central part of the disk” is not involved in the eclipses.

Lewis et al. (1993) proposed a qualitative model, wherein the O star forms a bow shock as it plows through the WR star’s

wind, to explain the observed variations in equivalent width and asymmetry of the WR emission lines as a function of phase.

In this article, we use 825 photometric observations made at the Sonoita Research Observatory (SRO) and the U.S.N.O. Flagstaff Station (NOFS), both in Arizona, from JD 2,453,609 to 2,454,279 to analyze the light curve and demonstrate the existence of intrinsic variability with a range between 0.05 and 0.1 mag, in addition to the stellar eclipses.

2. OBSERVATIONS

Our data fall into two sets. In the first set, two observations were made on each night with photometric sky conditions, for two seasons. The resulting data can be viewed as a long time series or folded onto the CX Cep ephemeris to display the eclipses. In the second data set, we sought to confirm interesting features in the light curves with time series.

The bulk of the observations were performed using the 0.35 m robotic telescope at SRO, with an SBIG STL 1001E CCD camera and Optec filters. Images were dark subtracted and flat-fielded using standard techniques in IRAF. A separate photometric pipeline based on algorithms from DAOPHOT (Stetson 1987) was used for aperture photometry; astrometry was performed using the UCAC astrometric reference catalog (Zacharias et al. 2004). Inhomogeneous ensemble photometry (Honeycutt 1992) was performed on the resulting star lists for CX Cep and four nearby constant stars (check stars). The check star data were used to correct for a known problem with scattered light in the telescope, which was repaired between the first and second CX Cep observing season. We have reprocessed the data from the first observing season, removing most of the scattered light effects. However, a small residual gradient remains in that data set. To complicate matters, the SRO telescope has a German Equatorial Mount; thus the CCD is inverted between negative and positive hour angle. Since the four check stars behave differently in this regard, we chose to ignore this complication and accept the slightly larger errors that result. Because check star 4 is the closest to CX Cep, we chose it to

determine the empirical offset between pre- and postrepair magnitudes. For the first season, check star 4 had a V magnitude of 11.562 with 160 data points. Following the repair, the V magnitude was 11.572, with 137 points, showing a difference of 0.010. Considering negative hour angle only, the difference is 0.0075 and, for positive hour angles only, it is 0.008. Based on this analysis, all CX Cep V magnitudes measured prior to the repair were increased by the difference, 0.008. CX Cep data were removed from consideration on nights when the check stars showed large deviations from their mean magnitude. Exposures were sufficiently long so that scintillation was not the dominant noise source.

The SRO 0.35 m telescope was also used to calibrate the CX Cep field at BVR_cI_c on several photometric nights. On each night, multiple standard stars from Landolt (1983, 1992) were observed with transformation and extinction coefficients determined. The comparison stars are listed in Table 1.

On one night, we used the 1.0 m telescope at NOFS to acquire a several-hour V -band time series with 40 s exposures. A SITe/Tektronix 2048 \times 2048 thinned, backside-illuminated CCD was used with 0.6763" pixels and a 23 \times 23' field of view.

In Figure 1, we present the BVR_I magnitudes, folded onto the epoch and period from Lipunova & Cherepashchuk, with the exception that, in order to accommodate all the available observations from 2,444,096 (Lipunova & Cherepashchuk 1982) to 2,454,194, it was necessary to increase the period slightly (from 2.12687 to 2.12691 days).

$$\phi = (\text{JD} - 2,444,451.4234)/2.12691$$

In the Figure, we can see (1) both primary and secondary minima, (2) ellipsoidal variation, (3) a somewhat asymmetric appearance, (4) increased scatter and complications between phases 0.7–0.9, and (5) more scatter overall than one might expect relative to the check stars.

The formal standard error from IRAF (0.003–0.004 mag units for most points) is about the size of the symbols on the figure. The (1 sigma) scatter is between 0.005 and

TABLE 1
CALIBRATION PHOTOMETRY FOR CX CEP AND ITS COMPARISON STARS. NUMBERS IN PARENTHESIS ARE STANDARD ERRORS.
COORDINATES ARE ACCURATE TO APPROXIMATELY 100 MAS

| Star | R.A. (deg) | Decl. (deg) | V | $B - V$ | $V - R$ | $V - I$ |
|--------------|---------------|----------------|----------------|---------------|---------------|---------------|
| CX Cep | 332.38935 | 57.74182 | 12.110 (0.044) | 0.811 (0.018) | 0.645 (0.011) | 1.292 (0.017) |
| 2 | 332.42129 | 57.76040 | 11.574 (0.023) | 0.656 (0.016) | 0.397 (0.012) | 0.805 (0.011) |
| 3 | 332.44942 | 57.79191 | 12.086 (0.020) | 0.463 (0.015) | 0.256 (0.011) | 0.566 (0.012) |
| 4 | 332.28191 | 57.80373 | 12.382 (0.020) | 0.544 (0.014) | 0.309 (0.017) | 0.648 (0.011) |
| 5 | 332.42557 | 57.82053 | 12.626 (0.019) | 0.864 (0.020) | 0.518 (0.011) | 1.051 (0.011) |
| 6 | 332.11352 | 57.82034 | 11.625 (0.017) | 0.542 (0.016) | 0.304 (0.012) | 0.630 (0.010) |
| 9 | 332.41171 | 57.66119 | 12.883 (0.021) | 0.787 (0.025) | 0.484 (0.013) | 0.960 (0.013) |
| 11 | 332.54646 | 57.60951 | 11.840 (0.017) | 0.447 (0.015) | 0.255 (0.012) | 0.564 (0.008) |
| 12 | 332.55132 | 57.85028 | 12.735 (0.014) | 0.693 (0.020) | 0.427 (0.013) | 0.905 (0.013) |
| 13 | 332.48071 | 57.83760 | 11.560 (0.017) | 0.339 (0.015) | 0.200 (0.011) | 0.447 (0.010) |

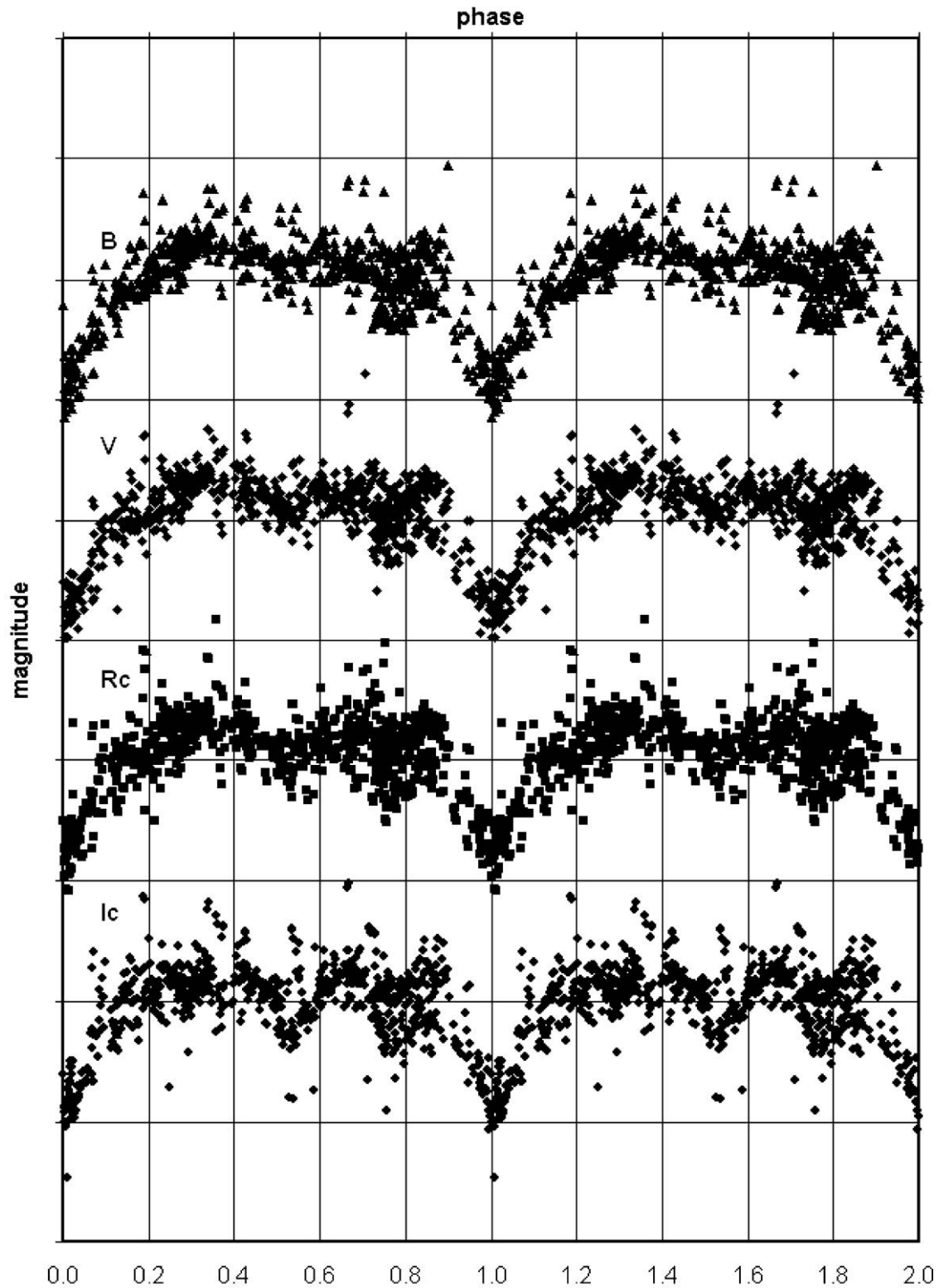


FIG. 1.—Four-color magnitudes for CX Cep. The magnitude division on the plot is 0.1.

0.009 mag for the check stars during various segments of the two seasons covered by data set one. By contrast, the data points during our time series on CX Cep (data set two), after the clearly bad data and the eclipsing variation were removed (see § 3), showed scatter ranging between 0.014 and 0.026 mag (with most about 0.022 mag) in V . We conclude (below) that the added factor of 3 in noise level must be due to intrinsic variability.

Between phases 0.7–0.9, the light curve shows increased scatter and additional attenuation. In spite of more noise even than at the other phases, there appear to be one extra minimum and an extra maximum in this region. We first sought to confirm the existence of these “features” by plotting each season’s data separately. The features still appeared, but with fewer data, they were more difficult to justify.

We then sought to confirm the features by conducting time series at SRO on 14 nights, ranging in length from 1.45 hr (10 data points) to 2.34 hr (69 data points), along with the one NOFS series of 69 points (over 2.5 hr), in V only, mentioned earlier. The time series data were taken close to the “monsoon season” in Arizona, so some data had to be rejected because of poor sky conditions (extralarge error bars and deviant values). The features remained.

3. MODELING

Lipunova & Cherepashchuk (1982) modeled the CX Cep system using the rectified light curve method and assuming that the minima were entirely due to eclipses of and by the extended atmosphere (see also Lamontagne et al. 1996) of the WR component. Our light curves show, however, rather distinct minima, suggesting grazing eclipses by a body with at least somewhat distinct edges. Our modeling was done using the PHOEBE interface (Prsa & Zwitter 2005) to the Wilson-Devinney (WD) code (Wilson & Devinney 1971). PHOEBE does not support computation of partially transparent stars. We were interested to find out how well we could fit the light curves using the standard eclipsing binary model. For the fitting, we used binned fluxes in each color, with a bin width of 0.02 in phase. We also used the Lewis et al. radial velocity data.

We made two modifications to the data in order to get a better solution. First, we omitted the data between phases 0.72 and 0.90, which includes the complications mentioned in § 2, intending to evaluate their cause in a second attempt. Second, we noticed that the Lewis et al. radial velocities were always significantly larger in value for the secondary star (the WR) than the model. Holding fixed all the other parameters in an approximate solution, we solved for systemic velocity (γ) using only the O5 radial velocity points, yielding a value of -88.3 km s^{-1} . Doing the same with the WR radial velocity points, we obtained -3.1 km s^{-1} . On this basis, we subtracted the difference (85.2) from all the WR radial velocity points. We assume that the discrepancy is caused by the velocities having been measured using lines generated in a complex WR moving wind.

We assume T_{eff} for the O star to be 42,000 K (Cox 1999). To account for the overall asymmetry of the phase diagrams, we included a “star spot” on the O5 star. None of the spot parameters are constrained well enough from the data to be solved. We used a spot longitude of 290° , a spot radius of 65° , and a spot temperature factor of 1.011. (If one varies nothing else in the solution, the temperature factor varies slightly with bandpass, being 1.0113 in B , 1.0139 in V , 1.0164 in R , and 1.0053 in I . These results are confirmed by the less asymmetric appearance of the I curve.) Lewis et al. proposed a qualitative model of the CX Cep system that contained a “bow shock” at approximately this location, produced by the interaction between the winds of the two stars.

The geometry of the CX Cep system, with its barely grazing eclipses, is not ideal for constraining parameters. We solved for the other parameters (semimajor axis, component surface potentials, secondary effective temperature, and bandpass luminosities) for a set of eight different (constrained) inclinations from 57° to 64° . At both ends of this range, there were clearly visible problems with the light curve fit. Then, choosing a starting point in the middle of this range, for iterations including i , PHOEBE converged on a solution with $i = 61.1^\circ$. Table 2 lists the parameters. Figure 2 shows the fits. The binned data between phases 0.72 and 0.90 are shown, but were not used in the fits. Figure 3 shows the fit to the radial velocity data found in Lewis et al. (1993).

Emission lines from WR stars can significantly contaminate measurements made with wide-band filters such as UBV (Crowther, 2007), typically by 0.5 mag. Lipunova and Cherepashchuk (1982) state, however (without a reference), that in the visual range, emission lines account for no more than 10% of the integrated light in this case, presumably because the WR is the fainter of the two stars. Lipunova & Cherepashchuk (1982) use a third-light parameter of 0.07 to account for “the extended envelope radiating in emission lines.” If we do this, the preferred inclination is 61.6° instead of 61.1° . The light curve fits look similar. When included among the free parameters, third light trades off with inclination; by 65° , however, the predicted

TABLE 2
ECLIPSING BINARY SYSTEM MODEL PARAMETERS

| | CX Cep, best PHOEBE solution | | |
|------------------------|------------------------------|----------------|----------------|
| | System | O5 | WN5 |
| INCL | 61.1 (0.71) | | |
| SMA | 27.8 (0.62) R_\odot | | |
| RM | 0.72 (0.022) | | |
| T_{eff} | | (42,000 K) | 19,700 (645) K |
| Potential | | 4.01 (0.064) | 4.02 (0.095) |
| Omega | | 3.28 | 2.87 |
| Mass | | 36.8 M_\odot | 26.4 M_\odot |
| Radius | | 8.5 R_\odot | 7.0 R_\odot |

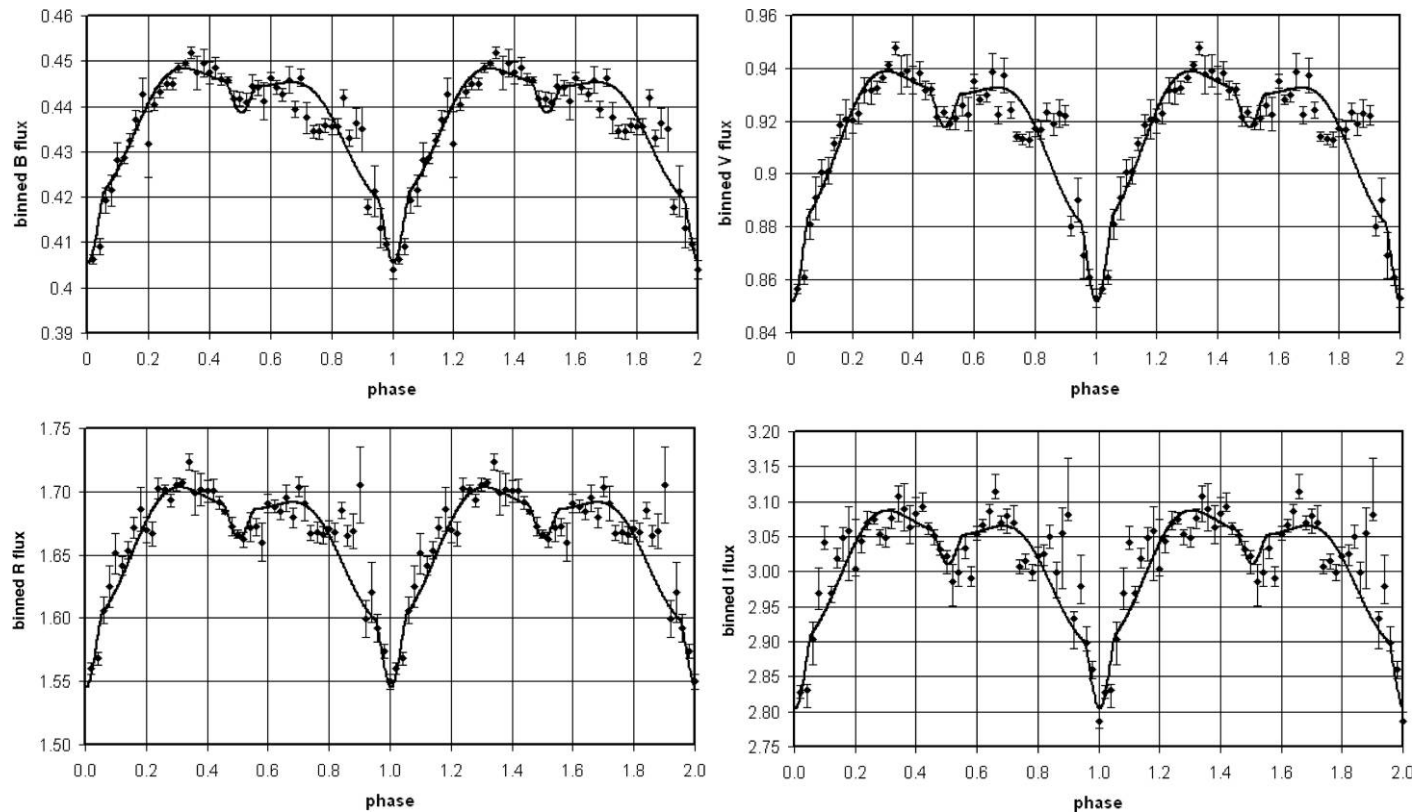


FIG. 2.—Binned data in each color. The error bars are standard errors computed from the data values in each bin. The solid line represents PHOEBE’s best fit. Each flux is computed relative to magnitude 12.0.

minima become too deep for the data, and the WR component becomes untenably small and cool. Qualitatively speaking, atmospheric eclipsing would require a lower value of i than the PHOEBE model would, in order to reproduce the observed shallow minima. So i cannot be very much larger than our value of 61.1° . Our preferred i is thus larger than $53 \pm 3^\circ$ determined by Lipunova and Cherepashchuk, but not as large as the 65° (Villar-Sbaffi et al. 2006) to 74° (Schulte-Ladbeck & van der Hucht 1989) required by the polarization studies.

Acceptable solutions seem to exist between $i = 58^\circ$ and 63° . These solutions yielded masses between 35.3 and 41.9 (best fit 37.2) M_\odot for the O5 star, and between 24.8 and 28.7 (best fit 26.8) M_\odot for the WN5 star.

The low effective temperature in the solution for the WR, which is especially poorly constrained in the solution, was surprising to us. Given the standard “opaque star” model, however, the shallowness of the secondary minimum requires this low temperature. However, in the case of a WR, the $\tau = 1$ radius approximated by the WD model is expected to be in the moving wind somewhere (Crowther 2007).

We were unable to model the unusual features in the data between phases 0.7 and 0.9. We note, however, that EE Cep has shown qualitatively similar behavior, more apparent in

the color index $B - I$, but seen also in the B light curve (Galan et al. 2008). One of the components of EE Cep is an invisible object at the center of a disk. Successful modeling of the irregular features requires a hole in the center of the disk. We conclude the reproducing this part of the CX Cep light curves may require extra material in the system not present in the PHOEBE binary model.

4. VARIABILITY

The data from Lipunova & Cherepashchuk have a similar scatter to ours, which we attribute to “physical variability” several times larger than their stated error bars.

On a longer time scale, we notice that the secondary minimum in the light curves published by Lipunova & Cherepashchuk (1982) for the 1970s is more prominent than it is with ours. Otherwise, the curves look very similar, even to the extent of showing the same asymmetry. If we free two parameters only, the potential and effective temperature of the WR, PHOEBE can nicely fit the earlier light curves (Fig. 4). The results show a higher temperature ($29,500 \pm 1800$ K rather than 19,700 K) and a larger radius ($8.0 R_\odot$ rather than 7.0). Remembering that we are probably looking at the variable appearance of the WR

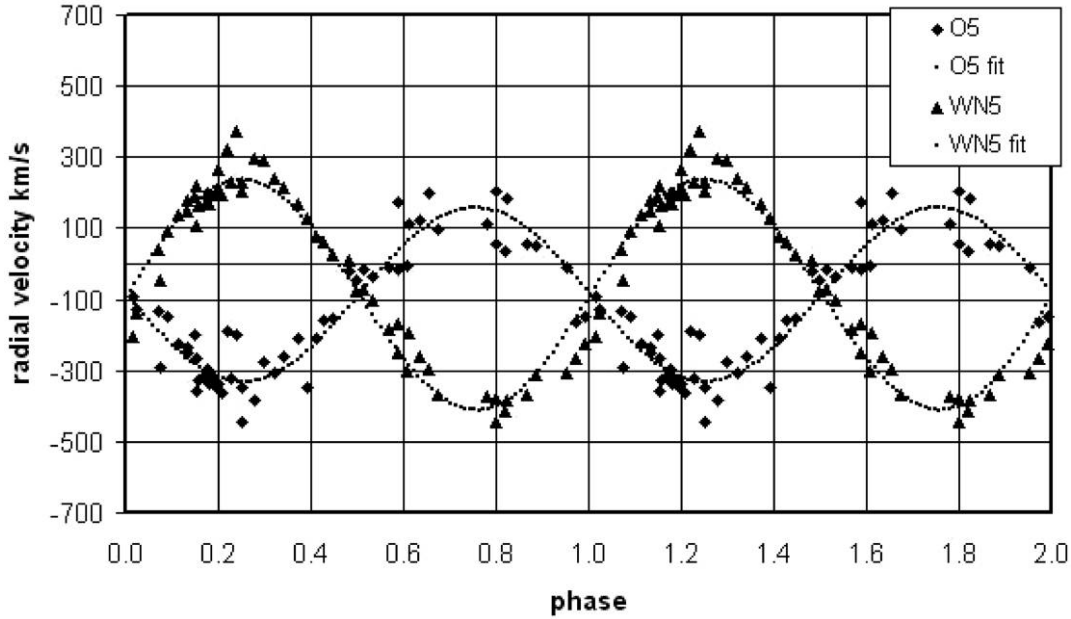


FIG. 3.—PHOEBE's fit to Lewis et al. (1993) radial velocity data, adjusted as described in the text.

wind and not an actual stellar surface, we can only say that noticeable changes seem to have occurred that involve the apparent size and energy output.

In Figure 5, we plot the $O - C$ residuals relative to the PHOEBE fit, in V band, as a function of time. The same plots for the other color bands look very similar. Clear time variability

can be seen, at the 10–12% level in the flux. Also, the scatter in the data is at least 2% in flux, which corresponds to about 0.02 mag difference. The high scatter in the phase diagrams across the whole gamut of phase must indicate that the variations are uncorrelated with and unaffected by the eclipsing binary aspects of the system.

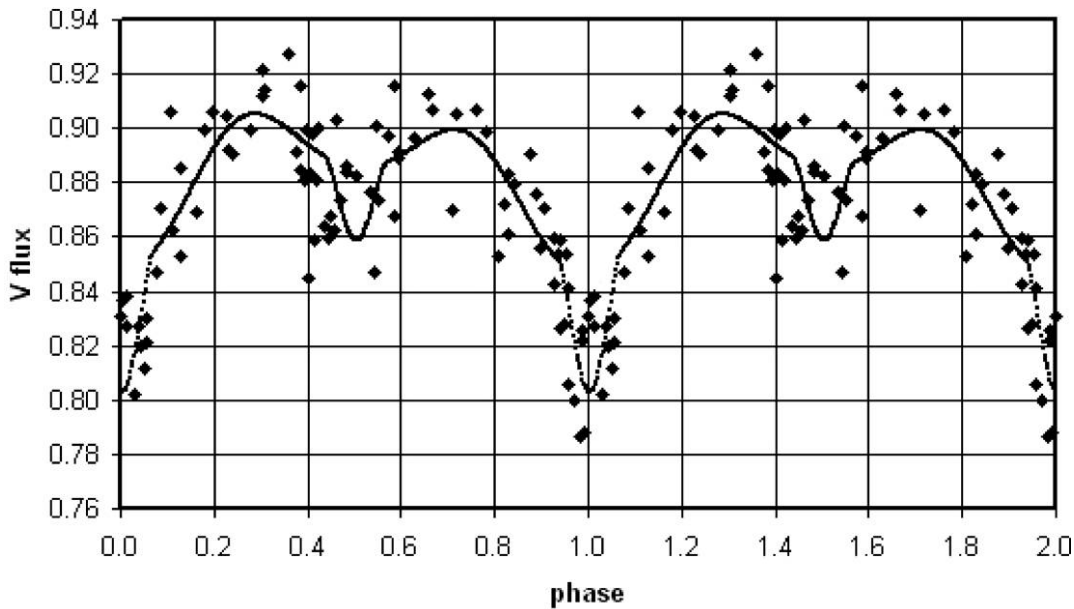


FIG. 4.—PHOEBE's fit to Lipunova & Cherepashchuk (1982) data for V .

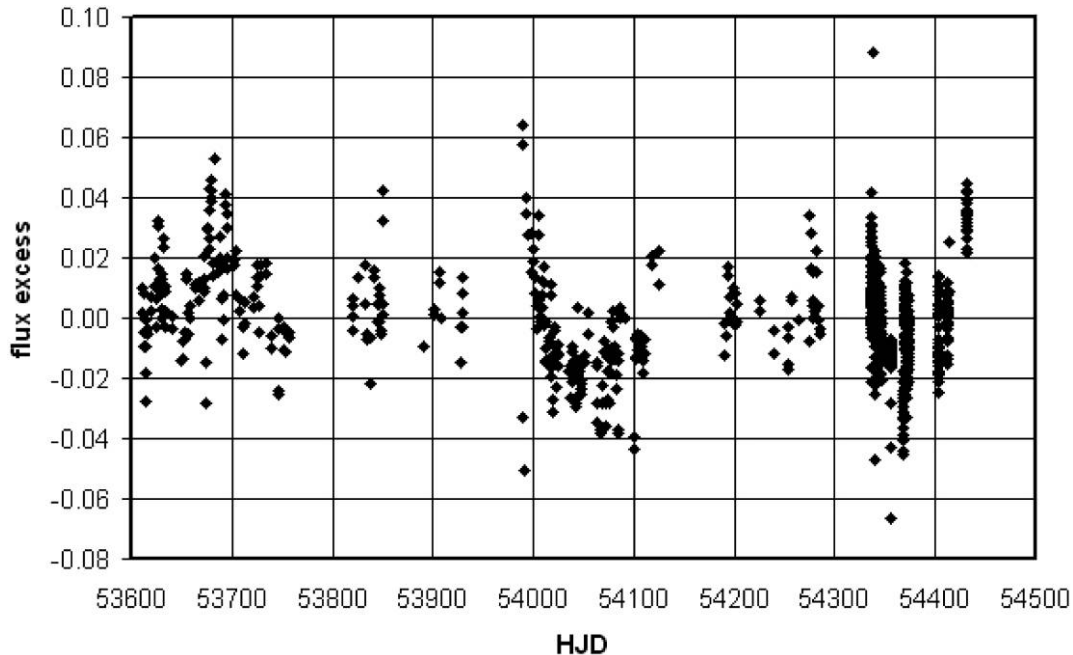


FIG. 5.—Flux residuals ($O - C$) relative to the PHOEBE fit, for each color, showing time variations in the system.

5. CONCLUSIONS

In summary, we were able to get a reasonable solution without invoking the complexity of atmospheric eclipse analysis. The secondary star in the light curve analysis approximates the optically thick portion of the WR star, which is presumed to be in the wind and not the surface of the hydrostatic star. The WD code fits the general features of the light curves and radial velocity curves, with reasonable solutions between $i = 58^\circ$ and $i = 63^\circ$, with a preferred value of $i = 61.1^\circ$. Our preferred inclination is larger than those previously published from light curve analysis, but still not as large as is required by the polarization data. The system is a detached binary. The semimajor axis ranges from 27 to 29 R_\odot , depending on i . Similarly, the mass ratio varies from 0.68 to 0.70. The WR “temperature” is much cooler than the O5, ranging from 19,000 K to 23,650 K in the various model fits (assuming 42,000 K for the O5 component). Although probably unphysical, this low value is required by the shallow secondary eclipses.

The range of models for the O5 component indicates a mass somewhere between 35 and 42 M_\odot , and a radius between 8.3 and 9.1 R_\odot . Similarly, the WR component has a mass between 24 and 29 M_\odot , and a radius between 6.3 and 8.4 R_\odot .

There is an asymmetry in the light curves, variable with wavelength, which can be modeled with a “spot” on the “leading edge” of the O5 star, where Lewis et al. (1993) hypothesized a bow shock to be similarly situated.

The light curves of Lipunova & Cherepashchuk (1982) look very similar to ours, including the asymmetry. Their secondary minimum is more prominent than ours, with a depth of about 0.04 instead of 0.02. We assume that some aspect of the size or optical depth of the WR wind configuration may have changed between 1974–80 and 2003–05.

The CX Cep system shows intrinsic variability of about 0.02 mag, which shows up as increased scatter in the phase diagrams (i.e., it is not related to the orbital motion). During the time period of 800 days covered by our observations, the $O - C$ residuals with respect to PHOEBE’s fitted light curve show variations with time.

The light curve “features” between phases 0.7–0.9 remain unexplained.

Two hot stars such as an O5 V and a WN5 should have $B - V$ of -0.43 . The observed $B - V$ of 0.82 implies a color excess of $E_{B-V} = 1.25$ and a total extinction of about 4.0 magnitudes. If we assume that $M_V = -6$, the CX Cep must lie at a distance of around 6300 pc.

REFERENCES

- Abbott, D. C., & Conti, P. S. 1987, ARA&A, 25, 133
 Cox, A. N. 1999, Astrophysical Quantities (New York: Springer)
 Crowther, P. A. 2007, ARA&A, 45, 177
 Galan, C., Mikolajewski, M., Tomov, T., & Cikala, M. 2008, Info. Bull. on Variable Stars, Commissions 27 & 42 of the IAU 5866
 Hiltner, W. A. 1948, AJ, 108, 56

- Honeycutt, R. K. 1992, *PASP*, 104, 435
- Lamontagne, R., Moffat, A. F. J., Drissen, L., Robert, C., & Matthews, J. M. 1996, *AJ*, 112, 2227
- Landolt, A. U. 1983, *AJ*, 88, 439
- . 1992, *AJ*, 104, 340
- Lewis, D., Moffat, A. F. J., Matthews, J. M., Robert, C., & Marchenko, S. V. 1993, *ApJ*, 405, 312
- Lipunova, N. A., & Cherepashchuk, A. M. 1982, *Soviet Astron.*, 26, 45
- Massey, P., & Conti, P. S. 1981, *ApJ*, 244, 169
- Moffat, A. F. J., Lamontagne, R., Shara, M. M., McAlister, & H. A. 1976, *AJ*, 91, 1392
- Prsa, A., & Zwitter, T. 2005, *AJ*, 628, 426
- Schulte-Ladbeck, R. E., & van der Hucht, K. A. 1989, *ApJ*, 337, 872
- Stetson, P. B. 1987, *PASP*, 99, 191
- Van der Hucht, K. A. 2001, *NewA Rev.*, 45, 135
- Villar-Sbaffi, A., St.-Louis, N., Moffat, A. F. J., & Piroola, V. 2006, *ApJ*, 640, 995
- Wilson, R. E., & Devinney, E. J. 1971, *AJ*, 166, 605
- Zacharias, N., Urban, S. E., & Zacharias, M. I., et al. 2004, *AJ*, 127, 3043